Serendipitous Discovery of Peptide Dialkyl Peroxides

by **Alessandro Moretto**, **Marta De Zotti**, **Laura Scipionato**, **Fernando Formaggio**, **Marco Crisma**, and **Claudio Toniolo***

Institute of Biomolecular Chemistry, CNR, Department of Organic Chemistry, University of Padova, I-35131 Padova (tel.: (+ 39) 049-827-5247; fax: (+ 39) 049-827-5239; e-mail: claudio.toniolo@unipd.it)

and

Sabrina Antonello and **Flavio Maran**

Department of Physical Chemistry, University of Padova, I-35131 Padova

and

Quirinus B. Broxterman

DSM Fine Chemicals, Advanced Synthesis and Catalysis, P.O. Box 18, 6160 MD Geleen, The Netherlands

Dedicated to Professor *Dieter Seebach* on the occasion of his 65th birthday

In an attempt to synthesize a homologous series of peptide peresters, we investigated the reaction of the oxazol-5(4*H*)-ones of Pht-(Aib)$_n$-OH ($n = 2-8$) and *tert*-butyl hydroperoxide in the presence of 4-(dimethylamino)pyridine. Unexpectedly, the major product isolated in each case proved to be the peptide dialkyl peroxide. This novel class of peptide derivatives was characterized by FT-IR, ^{1}H-NMR, MS, cyclic voltammetry, and X-ray diffraction. On the basis of the experimental data, a plausible mechanism is proposed for this reaction.

Introduction. – In the last few years, the study of intramolecular electron-transfer (ET) reactions in donor-spacer-acceptor (D-spacer-A) molecules has provided relevant information on how electrons are transferred through bonds and through space (solvent). We have recently investigated *intramolecular* ET reactions in systems in which A undergoes reductive cleavage of a σ-bond (dissociative electron transfer, DET). More specifically, as illustrated in *Scheme 1*, the phthalimido (Pht) moiety of Aib (α-aminoisobutyric acid), which is easily reduced to its radical anion, was selected as the donor D. In this system, the acceptor A is the Aib-O-O^{t}Bu perester function, a well-characterized dissociative-type acceptor [1]. Interestingly, we found in our electrochemical study that the DET rate of Pht-Aib-O-O^{t}Bu is several orders of magnitude lower than the adiabatic limit.

Scheme 1

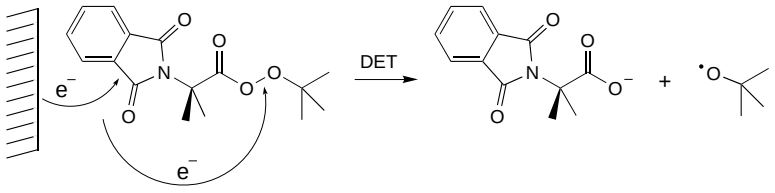

We also tackled the problem of the distance dependency of intramolecular DET processes. To achieve this goal, we decided to exploit rigid 3_{10}-helical peptide spacers [2] to control the electronic interaction between the D and A redox sites. Accordingly, since Aib homo-oligomers are known to fold into this ordered secondary structure [3][4], we planned the synthesis of the peptide perester series of type **I**. In the published syntheses of **I** ($n = 0$), activation of the COOH group and coupling of Pht-Aib-OH [5] was achieved *via* the corresponding acid chloride and pyridine [6], or, in higher yields, with 1-[3-(dimethylamino)propyl]-3-ethylcarbodiimide (EDC) and 4-(dimethylamino)pyridine (DMAP) [1], or with the acid chloride and DMAP [7]. It is reasonable to assume that all these methods lead to the predominant formation of an acylpyridinium intermediate [8] (in addition to a smaller amount of symmetrical anhydride [6][9]), which, in the presence of ^{t}BuOOH (*tert*-butyl hydroperoxide), would eventually afford the N^α-protected α-aminoacyl perester.

Any type of COOH activation of N^α-protected Aib homo-peptides overwhelmingly generates the corresponding oxazol-5(4*H*)-ones [10][11]. These reactive intermediates, in the presence of DMAP/^{t}BuOOH, were expected to afford the desired peptide peresters. In this paper, we show that, surprisingly enough, this reaction leads instead to a series of peptide dialkyl peroxides of type **II** as the major products.

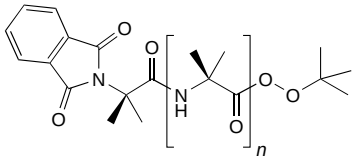

I

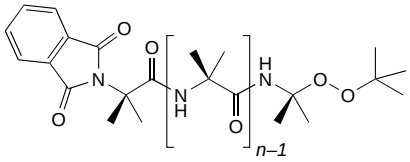

II

Results and Discussion. – *Peptide Synthesis.* The new N^α-blocked Aib derivatives and homo-peptide esters were prepared by known methodologies. In particular, Phac-Aib-O^{t}Bu (Phac = phenylacetyl) and Piv-Aib-O^{t}Bu (Piv = pivaloyl) were synthesized from H-Aib-O^{t}Bu [10] by the EDC/HOBt method [12] (HOBt = 1-hydroxy-1,2,3-benzotriazole) and the symmetrical anhydride method, respectively. The Pht-(Aib)$_n$-O^{t}Bu ($n = 2-8$) homo-peptide series was obtained either from Pht-Aib-Cl [13] and the pertinent H-(Aib)$_{n-1}$-O^{t}Bu [10] amino component in CH_2Cl_2 in the presence of (^{i}Pr)$_2$NEt or by the segment-condensation approach in MeCN using a peptide oxazol-5(4*H*)-one as the carboxy component [10][11][14][15]. The N^α-deprotected H-(Aib)$_{n-1}$-O^{t}Bu homo-peptides were prepared by catalytic hydrogenation of the corresponding benzyloxycarbonyl (Z) derivatives in MeOH [10]. The N^α-protected, C-terminally deprotected peptide acids [10][14] were obtained from the corresponding ^{t}Bu esters by treatment with dilute trifluoroacetic acid (TFA). The corresponding N^α-protected peptide oxazolones were synthesized by treatment of the N^α-protected peptide free acids with EDC in MeCN. The same synthetic steps were used to prepare

the oxazolone from Pht-Aib-[L-(α-Me)Val]$_2$-OH (Val = valine). The syntheses and characterizations of Z-Aib-OH [14][16], Piv-Aib-OH [17], Pht-Aib-OH [5], and Z-[L-(α-Me)Val]$_2$-O^{t}Bu [18] have already been reported.

Attempted Synthesis of Peptide Peresters. Three methods have been published for the synthesis of Pht-Aib-O-O^{t}Bu [1][6][7]. To prepare the higher homologues of the (Aib)$_n$ peptide perester series, we selected the method that exploits a carbodiimide (EDC) and a pyridine derivative (DMAP) to activate the COOH function, followed by addition of ^{t}BuOOH in CH_2Cl_2 (80% yield). The same approach was used to synthesize the Z-, Phac-, and Piv-N^α-blocked Aib derivatives. As mentioned above, in the presence of a carbodiimide, N^α-blocked Aib derivatives (except for Pht-Aib-OH) and peptides are known to afford the corresponding oxazol-5(4*H*)-ones [10][11]. These compounds were either isolated and characterized or prepared *in situ*. The X-ray diffraction structure of the oxazol-5(4*H*)-one of Pht-(Aib)$_2$-OH, solved in this work, is shown in *Fig. 1*. For a comparison with the crystal structures of other oxazolones of Aib-containing peptides and Pht-N^α-blocked Aib derivatives, see [19] and [9], respectively.

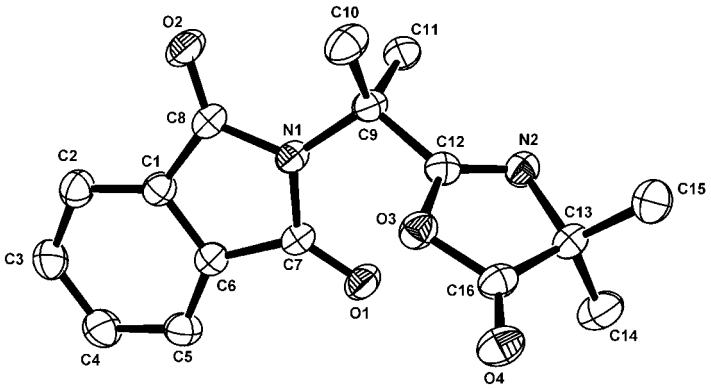

Fig. 1. *X-Ray crystal structure* (ORTEP view) *and numbering of the oxazol-5(4*H*)-one of Pht-(Aib)$_2$-OH.* Displacement ellipsoids are shown at the 30% probability level.

All our experiments led to a major final product that was purified by flash chromatography. However, yields were modest (25–40%), except for the Z-Aib derivative (68%). These compounds give rise to a reddish TLC spot when exposed to $NH_4SCN/FeSO_4/H_2SO_4$ [20][21], which is typical for peroxy-containing compounds.

Characterization of Peptide Dialkyl Peroxides. The putative N^α-blocked Aib derivative and homo-peptide peresters were characterized by a number of analytical and physico-chemical techniques, including FT-IR, ^{1}H-NMR, MS, cyclic voltammetry, and X-ray diffraction. The FT-IR absorption spectra of the Pht- and Z-protected amino acid and peptide derivatives (KBr pellets) are complex in the carbonyl stretching region and dominated by the contributions of the imide (two widely separated bands at 1780–1750 cm^{-1} and 1720–1700 cm^{-1}) and urethane (*ca.* 1720 cm^{-1}) absorptions, respectively [22] (*Table 1*). However, in each of the simpler spectra of the Piv- and Phac-derivatives, a single amide band is observed near 1660 cm^{-1}. In other words, no

evidence was obtained for the presence of a carbonyl stretching band indicative of the perester function (1820–1750 cm^{-1}) [22] in these two compounds.

The ^{1}H-NMR resonances associated with the Me protons of the ^{t}BuO group of the major reaction products (peroxides) in CD_3CN are listed in *Table 2* and compared with those of the corresponding esters. While the latter are found at 1.43–1.35 ppm, the former appear more upfield, between 1.19 and 1.11 ppm. Interestingly, the corresponding signal for the perester Pht-Aib-O-O^{t}Bu is displayed in an intermediate region (1.25 ppm). These findings further indicate that the major reaction products are distinct compounds from esters and peresters.

Mass-spectral analysis afforded more informative data. All experimentally determined molecular weights were consistently 28 mass units lower than calculated for the putative peptide peresters (*Table 3*).

The chemical structures of the new compounds were finally solved by X-ray diffraction analysis. We were able to grow suitable single crystals of the Pht-$(Aib)_3$ derivative under two different conditions, namely by vapour diffusion from $CHCl_3$/petroleum ether and by slow evaporation from MeOH. In *Figs. 2* and *3*, the X-ray structures of Pht-$(Aib)_2$-NH-C$(Me)_2$-O-O^{t}Bu and of an artifact thereof, [2-(methoxycarbonyl)]Bz-$(Aib)_2$-NH-C$(Me)_2$-O-O^{t}Bu (Bz = benzoyl), are depicted, the latter resulting from prolonged exposure to MeOH (alcoholysis of the phthalimide protecting group). However, the most interesting observation is that the reaction product differs from the putative tripeptide perester in the sense that the C-terminal C=O moiety is missing. Therefore, *the resulting product is an* N$^{\alpha}$*-blocked Aib homopeptide dialkyl peroxide*. This finding is in full agreement with all our physico-chemical and analytical investigations discussed above.

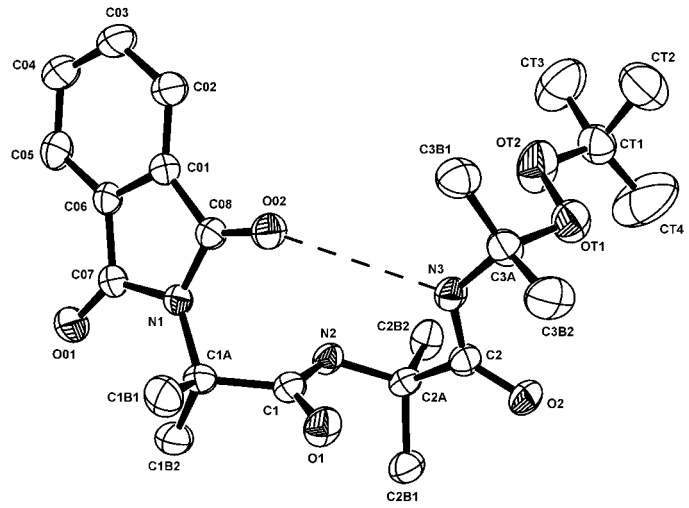

Fig. 2. *X-Ray crystal structure* (ORTEP view) *and numbering of Pht-(Aib)$_2$-NH-C(Me$_2$)-O-O^{t}Bu*. Displacement ellipsoids are shown at the 30% probability level. An intramolecular C=O···H–N H-bond is indicated by a dashed line.

Table 1. *Physical and Analytical Properties of Synthesized Peptides* (for abbreviations and conventions, see text and *Exper. Part*)

Compound	M.p. [°]	Recryst. solvent	TLC			IR [cm^{-1}]
			R_fI	R_fII	R_fIII	
Phac-Aib-O^{t}Bu	83 – 84	AcOEt/PE	0.80	0.95	0.60	3305, 1730, 1643, 1541
Phac-Aib-OH	177 – 178	EtOH/Et_2O	0.35	0.85	0.20	3374, 1722, 1613, 1540
Piv-Aib-O^{t}Bu	82 – 83	AcOEt/PE	0.85	0.95	0.75	3384, 1736, 1716, 1650, 1522
Pht-(Aib)$_2$-O^{t}Bu	oil	AcOEt/PE	0.90	0.95	0.65	3387, 1775, 1713, 1681, 1517
Pht-(Aib)$_2$-OH	208 – 209	EtOH/Et_2O	0.60	0.85	0.35	3401, 1775, 1745, 1702, 1649, 1521
Oxazol-5(4*H*)-one of Pht-(Aib)$_2$-OH	85 – 86	Et_2O/PE	0.95	0.95	0.65	1818, 1777, 1708, 1679
Pht-(Aib)$_3$-O^{t}Bu	97 – 98	AcOEt/PE	0.75	0.95	0.50	3374, 1776, 1705, 1683, 1653, 1535
Pht-(Aib)$_3$-OH	210 – 211	EtOH/Et_2O	0.50	0.95	0.20	3362, 1778, 1718, 1684, 1647, 1514
Pht-(Aib)$_4$-O^{t}Bu	135 – 136	AcOEt/PE	0.70	0.85	0.40	3351, 1776, 1712, 1682, 1665, 1526
Pht-(Aib)$_4$-OH	221 – 222	EtOH/Et_2O	0.40	0.80	0.15	3353, 3311, 1775, 1707, 1666, 1528
Pht-(Aib)$_5$-O^{t}Bu	195 – 196	AcOEt/PE	0.70	0.85	0.35	3359, 3339, 1776, 1710, 1670, 1523
Pht-(Aib)$_5$-OH	238 – 239	EtOH/Et_2O	0.35	0.80	0.15	3366, 1776, 1737, 1682, 1668, 1517
Pht-(Aib)$_6$-O^{t}Bu	229 – 230	AcOEt/PE	0.65	0.85	0.35	3334, 1776, 1731, 1712, 1666, 1527
Pht-(Aib)$_6$-OH	279 – 280	EtOH/Et_2O	0.30	0.75	0.10	3319, 1777, 1721, 1710, 1659, 1531
Pht-(Aib)$_7$-O^{t}Bu	182 – 183	AcOEt/PE	0.65	0.85	0.35	3326, 1777, 1731, 1712, 1662, 1529
Pht-(Aib)$_7$-OH	260 – 261	EtOH/Et_2O	0.25	0.75	0.10	3392, 3351, 1778, 1721, 1709, 1680, 1663, 1529
Pht-(Aib)$_8$-O^{t}Bu	248 – 249	AcOEt/PE	0.65	0.85	0.35	3323, 1777, 1709, 1664, 1529
Pht-(Aib)$_8$-OH	> 300	EtOH/Et_2O	0.20	0.75	0.10	3380, 3367, 1775, 1739, 1713, 1687, 1674, 1661, 1646, 1529
Pht-Aib-[L-(α-Me)Val]$_2$-O^{t}Bu	oil	AcOEt/PE	0.80	0.95	0.90	3388, 1779, 1715, 1680, 1662, 1653, 1522
Pht-Aib-[L-(α-Me)Val]$_2$-OH	102 – 103	EtOH/Et_2O	0.50	0.90	0.45	3389, 1777, 1710, 1678, 1656, 1509
Pht-Aib-NH-C(Me_2)-O-O^{t}Bu	oil	AcOEt/PE	0.90	0.95	0.60	3445, 3383, 1778, 1725, 1710, 1611, 1546
Pht-(Aib)$_2$-NH-C(Me_2)-O-O^{t}Bu	143 – 144	AcOEt/PE	0.85	0.95	0.55	3401, 3301, 1780, 1715, 1692, 1668, 1616, 1522
Pht-(Aib)$_3$-NH-C(Me_2)-O-O^{t}Bu	oil	AcOEt/PE	0.80	0.95	0.50	3379, 1776, 1710, 1676, 1527
Pht-(Aib)$_4$-NH-C(Me_2)-O-O^{t}Bu	98 – 99	AcOEt/PE	0.70	0.90	0.45	3320, 1778, 1710, 1667, 1525
Pht-(Aib)$_5$-NH-C(Me_2)-O-O^{t}Bu	272 – 273	AcOEt/PE	0.70	0.90	0.45	3333, 1777, 1721, 1711, 1667, 1528

Table 1 (cont.)

Compound	M.p. [°]	Recryst. solvent	TLC			IR [cm^{-1}]
			R_fI	R_fII	R_fIII	
Pht-(Aib)$_6$-NH-C(Me$_2$)-O-O^{t}Bu	297–298	AcOEt/PE	0.65	0.90	0.40	3321, 1777, 1712, 1663, 1529
Pht-(Aib)$_7$-NH-C(Me$_2$)-O-O^{t}Bu	156–158	AcOEt/PE	0.65	0.90	0.40	3313, 1779, 1712, 1663, 1532
Phac-NH-C(Me$_2$)-O-O^{t}Bu	85–86	AcOEt/PE	0.95	0.95	0.85	3299, 1660, 1560
Piv-NH-C(Me$_2$)-O-O^{t}Bu	57–58	AcOEt/PE	0.95	0.95	0.90	3353, 1658, 1537
Z-NH-C(Me$_2$)-O-O^{t}Bu	oil	AcOEt/PE	0.95	0.95	0.90	3389, 1727, 1531

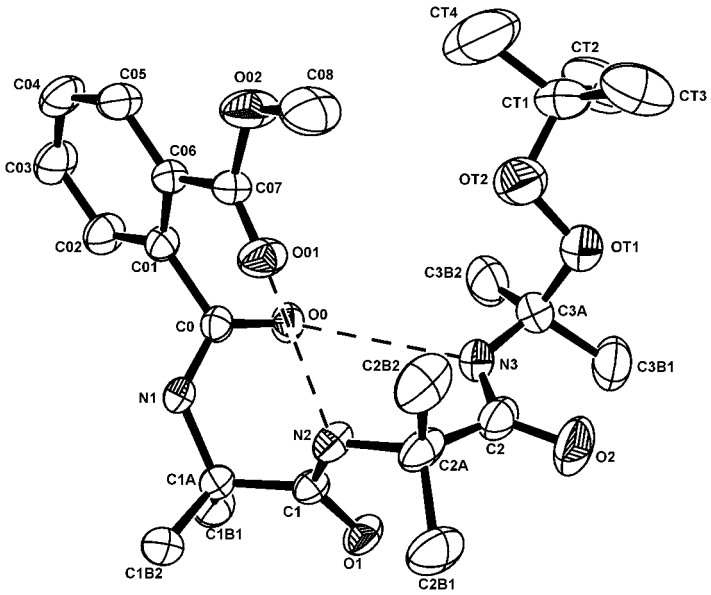

Fig. 3. *X-Ray crystal structure* (ORTEP view) *and numbering of [2-(methoxycarbonyl)]Bz-(Aib)$_2$-NH-C(Me$_2$)-O-O^{t}Bu*. Displacement ellipsoids are shown at the 30% probability level. Intramolecular C=O···H–N H-bonds are indicated by dashed lines.

Table 2. *^{1}H-NMR Chemical Shifts of the ^{t}Bu Groups of Synthesized Peptides in CD$_3$CN*

Esters	δ(^{t}Bu) [ppm]	Dialkyl peroxides	δ(^{t}Bu) [ppm]
Pht-(Aib)$_2$-O^{t}Bu	1.43	Pht-Aib-NH-C(Me$_2$)-O-O^{t}Bu	1.11
Pht-(Aib)$_3$-O^{t}Bu	1.36	Pht-(Aib)$_2$-NH-C(Me$_2$)-O-O^{t}Bu	1.18
Pht-(Aib)$_4$-O^{t}Bu	1.36	Pht-(Aib)$_3$-NH-C(Me$_2$)-O-O^{t}Bu	1.14
Pht-(Aib)$_5$-O^{t}Bu	1.35	Pht-(Aib)$_4$-NH-C(Me$_2$)-O-O^{t}Bu	1.16
Pht-(Aib)$_6$-O^{t}Bu	1.37	Pht-(Aib)$_5$-NH-C(Me$_2$)-O-O^{t}Bu	1.15
Pht-(Aib)$_7$-O^{t}Bu	1.37	Pht-(Aib)$_6$-NH-C(Me$_2$)-O-O^{t}Bu	1.16
Pht-(Aib)$_8$-O^{t}Bu	1.38	Pht-(Aib)$_7$-NH-C(Me$_2$)-O-O^{t}Bu	1.17
Phac-Aib-O^{t}Bu	1.35	Phac-NH-C(Me$_2$)-O-O^{t}Bu	1.17
Piv-Aib-O^{t}Bu	1.37	Piv-NH-C(Me$_2$)-O-O^{t}Bu	1.18
Z-Aib-O^{t}Bu	1.36	Z-NH-C(Me$_2$)-O-O^{t}Bu	1.19

Table 3. *Mass Spectral* (ESI-TOF) *Data for Peptide Dialkyl Peroxides*

Compound	$[M+Na]^+$	
	calc.	found
Pht-Aib-NH-C(Me_2)-O-O^{t}Bu	385.1734	385.1939
Pht-(Aib)$_2$-NH-C(Me_2)-O-O^{t}Bu	470.3390	470.2417
Pht-(Aib)$_3$-NH-C(Me_2)-O-O^{t}Bu	555.4088	555.2869
Pht-(Aib)$_4$-NH-C(Me_2)-O-O^{t}Bu	640.3317	640.3680
Pht-(Aib)$_5$-NH-C(Me_2)-O-O^{t}Bu	725.3844	725.4503
Pht-(Aib)$_6$-NH-C(Me_2)-O-O^{t}Bu	810.4372	810.5074
Pht-(Aib)$_7$-NH-C(Me_2)-O-O^{t}Bu	895.4900	895.5178
Pht-Aib-[L-(α-Me)Val]-[D,L-NH-C(Me)(^{i}Pr)]-O-O^{t}Bu[a])	526.2888	526.3066
Phac-NH-C(Me_2)-O-O^{t}Bu	254.1776	254.1807
Piv-NH-C(Me_2)-O-O^{t}Bu	288.1570	288.1668
Z-NH-C(Me_2)-O-O^{t}Bu	304.1532	304.1625

[a]) Mixture of diastereoisomers.

In both compounds, the characteristic peroxide O(T1)–O(T2) bond is only slightly shorter than in classical dialkylperoxides (1.46–1.48 Å) (*cf. Table 4*) [23]. Both compounds adopt a type III (III′) β-turn conformation [24–26], *i.e.*, the partial structure of the 3_{10}-helix [2], as expected for Aib homopeptides [3][4]. The C-terminal NH-C(Me)$_2$-O-O^{t}Bu residue is also folded, but the signs of its backbone torsional angles are opposite with respect to those of the preceding amino acids. The β-turn structure of the Pht-protected peptide is stabilized by one weak intramolecular C=O···H–N H-bond (3.284(4) Å) [27]. The Bz-containing peptide exhibits two such H-bonds, with distances of 2.972(5) and 3.216(4) Å, respectively. It is worth mentioning that these two X-ray structures are quite promising for the further exploitation of (Aib)$_n$ homopeptides as rigid molecular rulers in the study of the Pht/dialkyl peroxide DET processes.

Further evidence as to the chemical nature of our new compounds was obtained from cyclic voltammetry. The reduction of Piv-NH-C(Me)$_2$-O-O^{t}Bu is characterized by an irreversible and broad signal at 0.2 V s^{-1}, with a peak potential (E_p) of – 2.26 V. The main voltammetric features, *e.g.*, the peak width and shift of E_p as a function of scan rate, point to a very slow, heterogeneous ET process. As for many other peresters and dialkyl peroxides [28], the analysis of the voltammetric data is in agreement with a mechanism in which ET and fragmentation of the O–O bond are concerted. Such a fragmentation leads to the carboxylate or the alcoholate anion along with the alkoxy radical, *e.g.*, ^{t}BuO$^\bullet$, which is rapidly reduced (overall two-electron process). In *Fig. 4*, the voltammetric curves of Piv-NH-C(Me)$_2$-O-O^{t}Bu (curve *b*) and of two reference compounds, Piv-O-O^{t}Bu ($E_p = -1.55$ V (curve *a*) [1]) and di(*tert*-butyl) peroxide ($E_p = -2.50$ V (curve *c*) [29]) are shown. Our measurements are consistent with the fact that dialkyl peroxides are reduced at potentials more negative than *ca.* – 1.9 V, whereas peresters are reduced at potentials more positive than – 1.6 V [28]. Interestingly, the α-N-atom of the dialkyl peroxide lowers the reduction potential by more than 0.2 V (*cf.* curve *b vs. c*). In summary, cyclic voltammetry confirmed that the Piv-'Aib'-derivative (and by extension all other Aib derivatives and peptides synthesized in this work) are terminated by a dialkyl peroxide rather than by a perester function.

Table 4. *Selected Bond Lengths, Bond Angles, and Torsional Angles of Pht-(Aib)$_2$-NH-C(Me$_2$)-O-O^{t}Bu* (*cf. Fig. 2*) *and [2-(Methoxycarbonyl)]Bz-(Aib)$_2$-NH-C(Me$_2$)-O-O^{t}Bu* (*cf. Fig. 3*)

Parameter	Pht-(Aib)$_2$-NH-C(Me$_2$)-O-O^{t}Bu	[2-(methoxycarbonyl)]Bz-(Aib)$_2$-NH-C(Me$_2$)-O-O^{t}Bu
Bond lengths [Å]		
C(3A)–O(T1)	1.428(5)	1.476(7)
O(T1)–O(T2)	1.448(5)	1.436(7)
O(T2)–C(T1)	1.447(6)	1.399(8)
Bond angles [°]		
C(3A)–O(T1)–O(T2)	105.5(3)	109.2(4)
O(T1)–O(T2)–C(T1)	108.1(3)	108.6(5)
Torsional angles [°]		
C(0)–N(1)–C(1A)–C(1) ('ϕ_1')	– 48.1(5)	53.9(5)
N(1)–C(1A)–C(1)–N(2) (ψ_1)	– 46.2(5)	37.1(5)
C(1A)–C(1)–N(2)–C(2A) (ω_1)	– 161.5(3)	170.6(4)
C(1)–N(2)–C(2A)–C(2) (ϕ_2)	– 62.5(4)	63.9(5)
N(2)–C(2A)–C(2)–N(3) (ψ_2)	– 32.3(5)	25.3(6)
C(2A)–C(2)–N(3)–C(3A) (ω_2)	– 167.1(4)	166.7(5)
C(2)–N(3)–C(3A)–O(T1) ('ϕ_3')	61.6(5)	– 66.5(5)
N(3)–C(3A)–O(T1)–O(T2) ('ψ_3')	68.0(5)	– 69.0(5)
C(3A)–O(T1)–O(T2)–C(T1) ('ω_3')	– 176.0(4)	– 140.2(5)

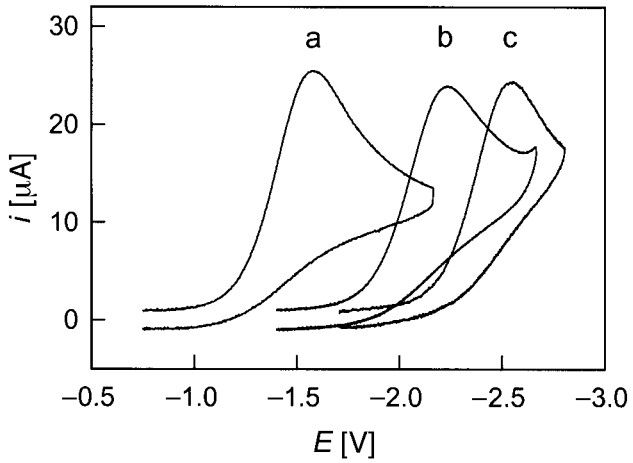

Fig. 4. *Cyclic voltammetry curves for the reduction of* a) *Piv-O-O^{t}Bu*, b) *Piv-NH-C(Me$_2$)-O-O^{t}Bu, and* c) *Bu^{t}O-O^{t}Bu in DMF.* Conditions: 0.1M Bu_4NClO_4, $T = 25°$, glassy C electrode (rel. to Standard Calomel Electrode), scan rate: 0.2 V s^{-1}, peptide concentration: 1 mM.

Mechanism of Peptide Dialkyl Peroxide Formation. We propose the following mechanism for the formation of peptide dialkyl peroxides (*Scheme 2*). Activation of the C-terminal COOH group of an N^{α}-blocked Aib homopeptide affords the corresponding oxazol-5(4*H*)-one [10][11]. Next, the pyridine N-atom of DMAP (the catalyst) attacks the oxazolone, which leads to an acylpyridinium intermediate [8][30][31]. It is

Scheme 2

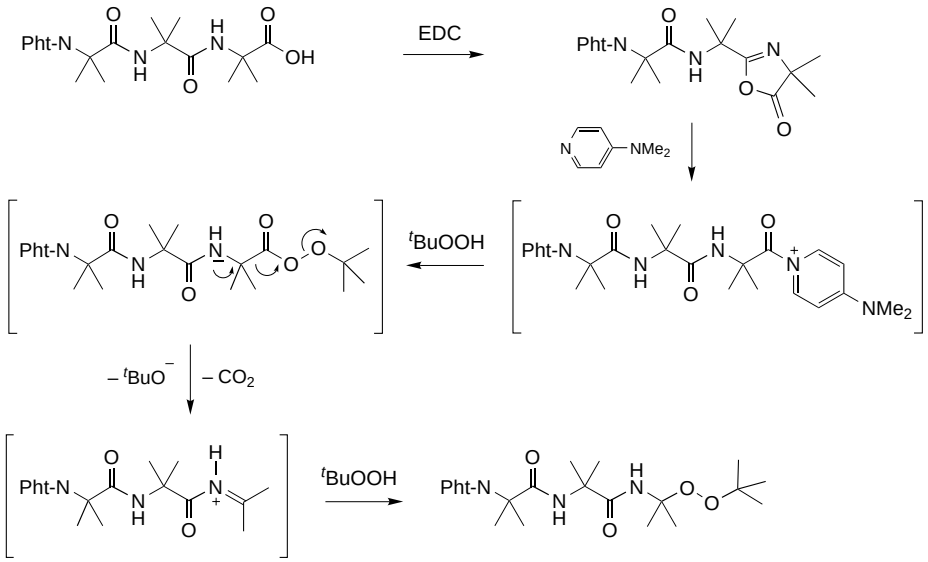

reasonable to assume that the weakly nucleophilic ^{t}BuOOH then attacks the terminal reactive C=O group of the acylpyridinium salt producing the peptide perester. If the latter is unstable, it might fragment heterolytically under loss of CO_2 and under formation of an iminium salt, as described by *Rüchardt* and co-workers [6][32]. In the final step, the iminium group is attacked by a second molecule of ^{t}BuOOH, which ultimately produces the peptide dialkyl peroxide.

To corroborate the proposed mechanism, we followed the progress of the reaction between the oxazolone of Z-Aib-OH and ^{t}BuOOH by HPLC-MS. *Fig. 5, a* depicts the chromatogram of the starting mixture in which the oxazolone **1** predominates. In *Fig. 5, b*, the latter has practically disappeared, with the concomitant onset of the peptide perester **2** and the imine **3**. Then, the peptide dialkyl peroxide **4** starts to form (*Fig. 5, c*), while, simultaneously, the peptide perester concentration decreases. In the final stage (*Fig. 5, d*), only the peptide dialkyl peroxide **4** is present to a significant extent.

Provided the planar iminium compound shown in *Scheme 2* is indeed an intermediate, then the utilization of a peptide substrate with *two* C-terminal, chiral α-amino acids should lead to epimerization and formation of a mixture of two diastereoisomeric peptide dialkyl peroxides. We, therefore, synthesized the tripeptide Pht-Aib-[L-(α-Me)Val]$_2$-OH. Due to the presence of the two C$^\alpha$-tetrasubstituted L-(α-Me)Val residues, epimerization *via* direct α-H abstraction can be excluded, but not *via* iminium salt formation. The ^{1}H-NMR and HPLC data shown in *Fig. 6* clearly indicate that a mixture of two diastereoisomeric peptide dialkyl peroxides was indeed obtained. The ^{1}H-NMR signal of the C-terminal NH group (the one closer to the center of epimerization) is split symmetrically (*Fig. 6, a*), and the same is true for the major HPLC peak (*Fig. 6, b*). Unfortunately, chromatographic separation of the two diastereoisomers was unsuccessful.

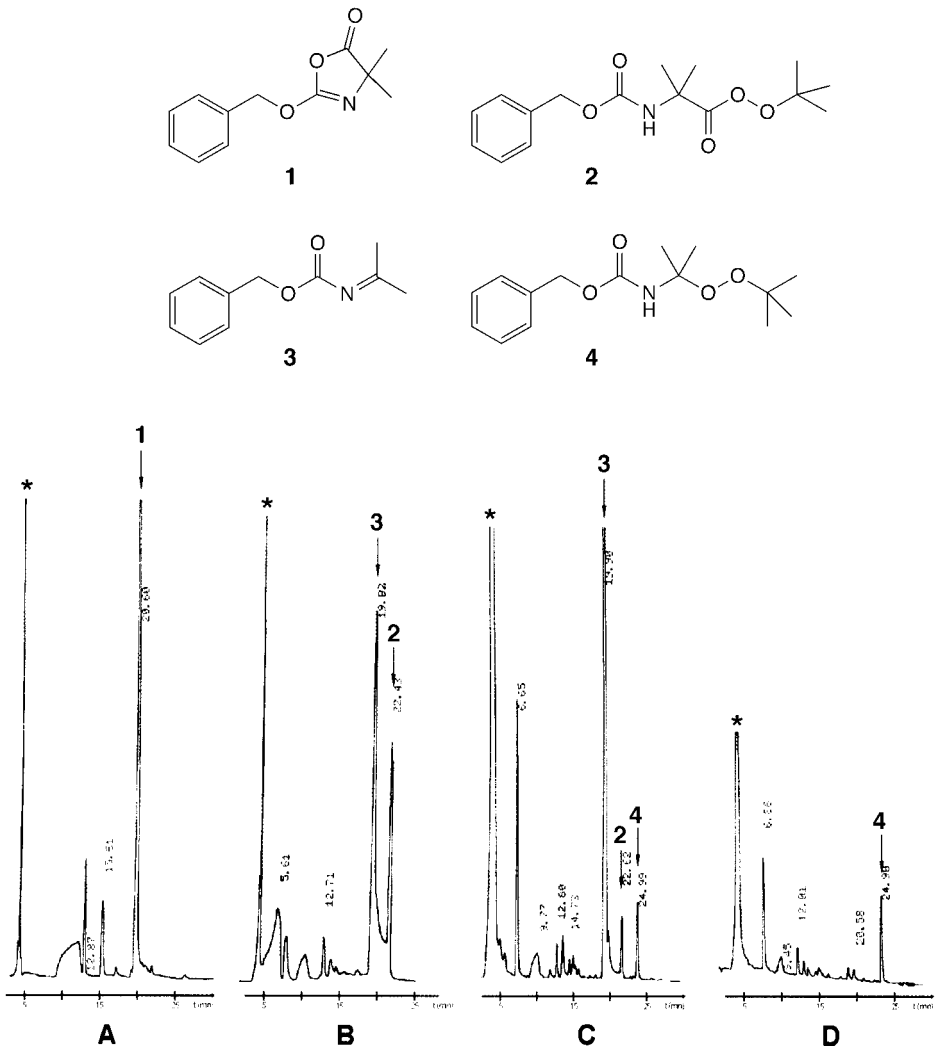

Fig. 5. *Progress of the reaction* **1** → **2** → **3** → **4** (analogous to the mechanism proposed in *Scheme 2*), *as followed by reversed-phase HPLC and MS*

Conclusions. – The original aim of our work was the preparation of Pht-N^{α}-protected Aib peptides with perester groups for probing the fine details of the dynamics of dissociative electron transfer (DET) processes [1]. However, our experiments clearly show that peptide peresters, although formed *in situ*, are not stable enough to be isolated or investigated. Since Pht-Aib-O-O^{t}Bu is fairly stable and can be easily synthesized [1][6][7], we tend to attribute the instability of the Aib-containing homologous peptide peresters to the presence of the C-terminal *α-amide* function. This assumption is corroborated by the observation that, among the N^{α}-blocked aminoacyl derivatives studied so far, only Pht-Aib-OH and racemic, *trans*-oriented N^{α}-phthaloyl-

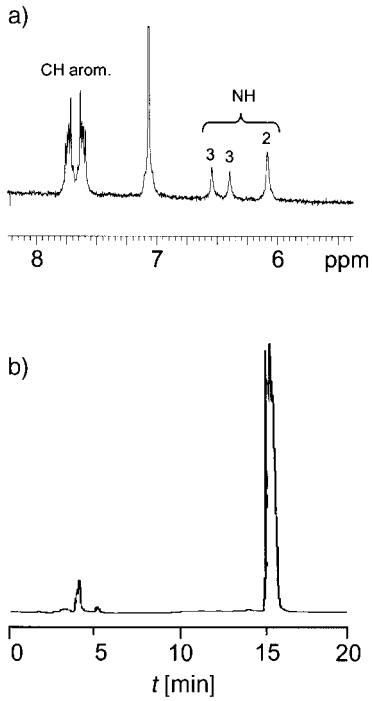

Fig. 6. *Characterization of the diastereoisomeric mixture of Pht-Aib-[*L*-(α-Me)Val]-[*D,L*-NH-C(Me)(*^{i}*Pr)]-O-O*^{t}*Bu*. *a*) Partial ^{1}H-NMR spectrum; *b*) analytical, reversed-phase HPLC chromatogram.

2-aminocyclohexanecarboxylic acid [33], which contain an *α-imide* or a *β-amide* function, respectively, afforded the desired peresters. Following this working hypothesis, we are currently trying to synthesize Pht-N^{α}-protected Aib homo-oligomeric peresters [33] that bear the above mentioned rigid *β*-amino acid residue [34][35] at the C-terminus. At the same time, we are also actively investigating DET processes and trying to solve the preferred three-dimensional structure of the peptide series based on the Pht/dialkyl peroxide dyad.

Experimental Part

General. Abbreviations: NMM (*N*-methylmorpholine), PE (petroleum ether), DMF (*N*,*N*-dimethylformamide), TFA (trifluoroacetic acid). Anal. TLC and prep. FC: silica gel F 254 plates and silica gel 60 (0.040–0.063 mm; *Merck*), resp.; TLC eluent systems: $CHCl_3$/EtOH 9:1 (R_fI); BuOH/AcOH/H_2O 3:1:1 (R_fII), and toluene/EtOH 7:1 (R_fIII); UV fluorescence detection (254 nm) or chlorine-starch-potassium iodide development. Anal. HPLC: C_{18} reversed-phase column *Vydac 218TP54* with a *Pharmacia LKB-LCC 2252* instrument equipped with a *Uvicord SD* ($\lambda = 226$ nm). M.p. determination with a temp. raise of 3°/min on a *Leitz Laborlux 12* apparatus; uncorrected. IR Spectra: KBr technique, *Perkin-Elmer 580-B* spectrophotometer equipped with a *Perkin-Elmer 3600* IR data station. ^{1}H-NMR Spectra (250 MHz): in CD_3CN (99.95% D; *Aldrich*) or (D_6)DMSO (99.96% D, *Acros Organics*); *Bruker AC-250* spectrometer; δ in ppm rel. to Me_4Si as internal standard. Mass spectra: *Mariner* ESI-TOF instrument (*Perseptive Biosystems*); positive and negative ions accelerated to 10, 15, 20, or 30 keV and analyzed in the linear mode. Electrochemical apparatus and procedures: DMF (99%, *Acros Organics*) was treated as previously described [29]. Electrochemical

measurements were conducted in an all-glass cell, thermostated at 25°. An *EG&G-PARC 173/179* potentiostat-digital coulometer, an *EG&G-PARC 175* universal programmer, and a *Nicolet 3091* 12-bit resolution digital oscilloscope were used. The feedback correction was applied to minimize the ohmic drop between the working and the reference electrodes. Experiments were carried out inside a double-wall copper *Faraday* cage. Glassy carbon, prepared and activated as previously described [29], was employed as the working electrode. The reference electrode was Ag/AgCl, calibrated after each experiment against the ferrocene/ferricenium couple, and finally converted to the KCl saturated calomel electrode. The counter electrode was a Pt plate (1 cm^2). To avoid father-son reaction between peroxide and ^{t}BuO$^-$ [36][37], one equivalent of acetanilide was added to the soln. Detailed procedures representative of each type of reaction exploited are described below.

Phac-Aib-O^{t}Bu. To an ice-cold soln. of Phac-OH (0.50 g, 2.26 mmol) in CH_2Cl_2 (5 ml), HOBt (0.30 g, 2.26 mmol) and EDC hydrochloride (0.43 g, 2.26 mmol) were added, followed by a soln. of H-Aib-O^{t}Bu [10] (obtained by catalytic hydrogenation of 0.76 g, 2.26 mmol, of the corresponding Z-protected synthetic precursor in MeOH) in CH_2Cl_2 (8 ml) and by NMM (0.28 ml, 2.26 mmol). The soln. was stirred at r.t. for 24 h and then evaporated to dryness. The residue was dissolved in AcOEt, and the resulting soln. was washed with 10% $KHSO_4$ soln., H_2O, 5% $NaHCO_3$ soln., and H_2O, dried (Na_2SO_4), filtered, and evaporated to dryness. The crude product was purified by FC and crystallized from AcOEt/PE. Yield: 91%.

Piv-Aib-O^{t}Bu. To H-Aib-O^{t}Bu (3.4 mmol, prepared as described above) in CH_2Cl_2 (10 ml), $(Piv)_2O$ (3.98 ml, 17.0 mmol) in CH_2Cl_2 (4 ml) was added. The soln. was stirred at r.t. for 4 h and evaporated several times to dryness by adding toluene to remove the excess of $(Piv)_2O$. The residue was crystallized from AcOEt/PE. Yield: 89%.

Pht-(Aib)$_2$-O^{t}Bu. Pht-Aib-Cl [13] (4.0 g, 16.5 mmol) was dissolved at 0° in CH_2Cl_2 (35 ml). Then, H-Aib-O^{t}Bu (16.5 mmol, prepared as described above) in CH_2Cl_2 (55 ml) and $(i\text{-}Pr)_2NEt$ (2 ml, 16.5 mmol) were added. The soln. was stirred at r.t. for 3 h and evaporated to dryness. The residue was dissolved in AcOEt, and the resulting soln. was washed with 10% $KHSO_4$ soln., H_2O, 5% $NaHCO_3$ soln., and H_2O, dried (Na_2SO_4), filtered, and evaporated to dryness. The crude product was purified by FC, dissolved in AcOEt, and precipitated by adding PE. Yield: 72%.

Pht-(Aib)$_2$-OH. Pht-$(Aib)_2$-O^{t}Bu (2.0 g, 5.20 mmol) was dissolved in a 1:1 mixture of TFA and CH_2Cl_2 (10 ml). The soln. was stirred at r.t. for 2 h. The solvent was evaporated several times to dryness by adding Et_2O to remove the excess of TFA. The crude product was dried over solid KOH *in vacuo* for 12 h and crystallized from EtOH/Et_2O. Yield: 90%.

*Oxazol-5(4*H*)-one from Pht-(Aib)$_2$-OH*. To an iced soln. of Pht-$(Aib)_2$-OH (0.50 g, 1.5 mmol) in MeCN (15 ml), EDC hydrochloride (0.30 g, 1.7 mmol) was added. The soln. was stirred at r.t. for 2 h and evaporated to dryness. The residue was dissolved in AcOEt, and the resulting soln. was washed with 10% $KHSO_4$ soln. and H_2O, dried (Na_2SO_4), filtered, and evaporated to dryness. The crude product was crystallized from Et_2O/PE. Yield: 91%.

Pht-(Aib)$_4$-O^{t}Bu. A soln. of the oxazol-5(4*H*)-one of Pht-$(Aib)_2$-OH (2.0 g, 6.1 mmol) and H-$(Aib)_2$-O^{t}Bu (obtained by catalytic hydrogenation of 2.3 g, 6.1 mmol of the corresponding Z-protected synthetic precursor in MeOH [38]) in MeCN (20 ml) was refluxed for 48 h and evaporated to dryness. The residue was dissolved in AcOEt, and the resulting soln. was washed with 10% $KHSO_4$ soln., H_2O, 5% $NaHCO_3$ soln., and H_2O, dried (Na_2SO_4), filtered, and evaporated to dryness. The crude product was crystallized from AcOEt/PE. Yield: 78%.

Pht-Aib-NH-C(Me)$_2$-O-O^{t}Bu. To an ice-cold soln. of the oxazol-5(4*H*)-one of Pht-$(Aib)_2$-OH (0.5 g, 1.5 mmol) in CH_2Cl_2 (5 ml), ^{t}BuOOH (2.9 ml of a 5.5M soln. in decane, 16.0 mmol) and DMAP (0.78 g, 6.4 mmol) were added. The soln. was refluxed for 24 h and evaporated to dryness. The residue was dissolved in AcOEt, and the resulting soln. was washed with 10% $KHSO_4$ soln., H_2O, 5% $NaHCO_3$ soln., and H_2O, dried over Na_2SO_4, filtered, and evaporated to dryness. The crude product was purified by FC and precipitated from an AcOEt soln. by adding PE. Yield: 32%.

X-Ray Diffraction. Colourless single crystals of the oxazol-5(4*H*)-one of Pht-$(Aib)_2$-OH, Pht-$(Aib)_2$-NH-$C(Me)_2$-O-O^{t}Bu, and [2-(methoxycarbonyl)]Bz-$(Aib)_2$-NH-$C(Me)_2$-O-O^{t}Bu were grown from Et_2O by slow evaporation, from $CHCl_3$/PE by vapour diffusion, and from MeOH by slow evaporation, resp. Intensity data were collected on a *Philips PW-1100* four-circle X-ray diffractometer and corrected for *Lorentz* and polarization effects. Data of Pht-$(Aib)_2$-NH-$C(Me)_2$-O-O^{t}Bu were additionally corrected for crystal decay, as suggested by monitoring of three standard reflections (max decay 62%). Graphite-monochromated CuK_α radiation ($\lambda = 1.54178$ Å) and $\theta - 2\theta$ scan-mode were used. Cell parameters were obtained by least-square refinements of the angular setting of 48 carefully centered high-angle reflections. The structures were solved by direct methods with the SHELXS 97 program [39]. Refinements were carried out by the full-matrix block least-squares procedure on F^2 with SHELXL 97 [40], with all non-H-atoms anisotropic, and allowing their positional

Table 5. *Crystallographic Data and Details of Structure Determinations for the Oxazol-5(4H)-one of Pht-(Aib)$_2$-OH, for Pht-(Aib)$_2$-NH-C(Me$_2$)-O-O^{t}Bu, and for [2-(Methoxycarbonyl)]Bz-(Aib)$_2$-NH-C(Me$_2$)-O-O^{t}Bu*

Parameter	Oxazolone of Pht-(Aib)$_2$-OH	Pht-(Aib)$_2$-NH-C(CH$_3$)$_2$-O-O^{t}Bu	[2-(Methoxycarbonyl)]Bz-(Aib)$_2$-NH-C(CH$_3$)$_2$-O-O^{t}Bu
Empirical formula	$C_{16}H_{16}N_2O_4$	$C_{23}N_{33}N_3O_6$	$C_{24}H_{37}N_3O_7$
M_r	300.3	447.5	479.6
Crystal system	orthorhombic	monoclinic	monoclinic
Space group	$P2_12_12_1$	$P2_1/n$	$P2_1$
a [Å]	9.652(2)	13.210(3)	9.333(3)
b [Å]	10.628(3)	10.703(3)	11.029(3)
c [Å]	15.008(3)	18.288(4)	13.547(4)
β [°]	90	103.89(4)	91.82(5)
V [Å^3]	1539.5(6)	2510.1(11)	1393.7(7)
Z	4	4	2
D [g cm^{-3}]	1.296	1.184	1.143
μ [mm^{-1}]	0.782	0.706	0.693
Radiation	CuK_α ($\lambda = 1.54178$ Å)	CuK_α ($\lambda = 1.54178$ Å)	CuK_α ($\lambda = 1.54178$ Å)
Crystal size [mm]	$0.60 \times 0.35 \times 0.30$	$0.50 \times 0.10 \times 0.10$	$0.45 \times 0.30 \times 0.20$
Mode of scan	$\theta - 2\theta$	$\theta - 2\theta$	$\theta - 2\theta$
$F(000)$	632	960	516
θ Range [°]	5.5 – 60.0	3.7 – 60.1	3.3 – 60.0
Index ranges	$-1 \le h \le 10$	$-14 \le h \le 14$	$-10 \le h \le 10$
	$0 \le k \le 11$	$0 \le k \le 12$	$0 \le k \le 12$
	$0 \le l \le 16$	$0 \le l \le 20$	$0 \le l \le 15$
Reflections collected	1487	3842	2288
Independent reflections	1462 (R(int) = 0.017)	3721 (R(int) = 0.019)	2194 (R(int) = 0.064)
Absorption correction	none	none	none
Refinement method	full-matrix block least-squares on F^2	full-matrix block least-squares on F^2	full-matrix block least-squares on F^2
Data, restraints, parameters	1462, 0, 200	3721, 18, 305	2194, 1, 307
Goodness-of-fit on F^2	1.129	1.038	1.080
Final R indices [$I > 2\sigma(I)$]	$R_1 = 0.0429$	$R_1 = 0.0824$	$R_1 = 0.0598$
	$wR_2 = 0.1104$	$wR_2 = 0.2276$	$wR_2 = 0.1750$
R Indices (all data)	$R_1 = 0.0434$	$R_1 = 0.1326$	$R_1 = 0.0651$
	$wR_2 = 0.1109$	$wR_2 = 0.2649$	$wR_2 = 0.1829$
Largest difference peak and hole [e Å^{-3}]	0.181, −0.247	0.301, −0.264	0.392, −0.235

and anisotropic displacement parameters to refine at alternate cycles. The H-atoms were calculated at idealized positions and refined by allowing them to ride on their carrying atom, with U_{iso} being 1.2 × (1.5 × for Me) as large as U_{eq} of the parent atom. The C-terminal ^{t}Bu group of Pht-(Aib)$_2$-NH-C(Me)$_2$-O-O^{t}Bu is distorted. Each of its three Me groups was refined on two sites, with population parameters of 0.52 and 0.48, respectively. Restraints were applied to the bond distances and angles of the disordered atoms. The relatively high final R factors might be ascribed in part to the crystal decay and possible additional disorder at the C-terminal ^{t}Bu group that could not be modeled satisfactorily. Crystallographic data and details of the structure determinations are presented in *Table 5*. Atomic coordinates, bond distances and angles, and anisotropic displacement parameters have been deposited with the *Cambridge Crystallographic Data Centre* (*CCDC*) as deposition No. CCDC 184554, 184555, and 184556. Copies of the data can be obtained, free of charge, on application to the *CCDC*, 12 Union Road, Cambridge CB21EZ, UK (fax: +44(1223)336033; e-mail: deposit@ccdc.cam.ac.uk).

This work was in part financially supported by the University of Padova (research project A.OEEO.97) and the *Ministero dell'Istruzione, dell'Università e della Ricerca* (*MIUR*) of Italy.

REFERENCES

[1] S. Antonello, F. Formaggio, A. Moretto, C. Toniolo, F. Maran, *J. Am. Chem. Soc*. **2001**, *123*, 9577.
[2] C. Toniolo, E. Benedetti, *Trends Biochem. Sci*. **1991**, *16*, 350.
[3] C. Toniolo, E. Benedetti, *Macromolecules* **1991**, *24*, 4004.
[4] C. Toniolo, M. Crisma, F. Formaggio, C. Peggion, *Biopolymers (Pept. Sci.)* **2001**, *60*, 396.
[5] D. Leibfritz, E. Haupt, N. Dubischar, H. Lachmann, R. Oekonomopulos, G. Jung, *Tetrahedron* **1982**, *38*, 2165.
[6] Ch. Rüchardt, G. Hamprecht, *Chem. Ber*. **1968**, *101*, 3957.
[7] A. Moretto, Ph.D. Thesis, University of Padova, 2001.
[8] E. F. V. Scriven, *Chem. Soc. Rev*. **1983**, *12*, 129.
[9] G. Valle, C. Toniolo, G. Jung, *Liebigs Ann. Chem*. **1986**, 1809.
[10] D. S. Jones, G. W. Kenner, J. Preston, R. C. Sheppard, *J. Chem. Soc*. **1965**, 6227.
[11] H. Brückner, in 'Chemistry of Peptides and Proteins', Eds. W. A. König, W. Voelter, Attempto, Tübingen, 1989, Vol. 4, p. 79.
[12] W. König, R. Geiger, *Chem. Ber*. **1970**, *103*, 788.
[13] S. Gabriel, *Ber. Dtsch. Chem. Ges*. **1911**, *44*, 57.
[14] M. T. Leplawy, D. S. Jones, G. W. Kenner, R. C. Sheppard, *Tetrahedron* **1960**, *11*, 39.
[15] H. Brückner, M. Currle, in 'Second Forum on Peptides', Eds. A. Aubry, M. Marraud, B. Vitoux, Libbey Eurotext, London, 1989, p. 251.
[16] G. Valle, F. Formaggio, M. Crisma, G. M. Bonora, C. Toniolo, A. Bavoso, E. Benedetti, B. Di Blasio, V. Pavone, C. Pedone, *J. Chem. Soc., Perkin Trans. 2* **1986**, 1371.
[17] R. J. L. Martin, C. H. Skovron, D. L. H. Yiu, *J. Chem. Soc., Perkin Trans. 2* **1974**, 125.
[18] A. Polese, F. Formaggio, M. Crisma, G. Valle, C. Toniolo, G. M. Bonora, Q. B. Broxterman, J. Kamphuis, *Chem.–Eur. J.* **1996**, *2*, 1104.
[19] C. Toniolo, M. Crisma, F. Formaggio, *Biopolymers (Pept. Sci.)* **1996**, *40*, 627.
[20] A. J. Martin, in 'Organic Analysis', Interscience, New York, 1960, Vol. 4, p. 1.
[21] S. Siggia, in 'Quantitative Organic Analysis', Wiley, New York, 1963, p. 255.
[22] L. J. Bellamy, in 'The Infrared Spectra of Complex Molecules', Methuen, London, 1966.
[23] F. A. Allen, O. Kennard, D. G. Watson, L. Brammer, A. G. Orpen, R. Taylor, *J. Chem. Soc., Perkin Trans. 2* **1987**, S-1.
[24] C. M. Venkatachalam, *Biopolymers* **1968**, *6*, 1425.
[25] C. Toniolo, *Crit. Rev. Biochem*. **1980**, *9*, 1.
[26] G. D. Rose, L. M. Gierasch, J. P. Smith, *Adv. Protein Chem*. **1985**, *37*, 1.
[27] C. H. Görbitz, *Acta Crystallogr., Sect. B* **1989**, *45*, 390.
[28] F. Maran, D. D. M. Wayner, M. S. Workentin, *Adv. Phys. Org. Chem*. **2001**, *36*, 85.
[29] S. Antonello, M. Musumeci, D. D. M. Wayner, F. Maran, *J. Am. Chem. Soc*. **1997**, *119*, 9541.
[30] J. Liang, J. C. Ruble, G. C. Fu, *J. Org. Chem*. **1998**, *63*, 3154.
[31] J.-P. Gamet, R. Jacquier, J. Verducci, *Tetrahedron* **1984**, *40*, 1995.
[32] Ch. Rüchardt, H. Schwarzer, *Chem. Ber*. **1966**, *99*, 1878.
[33] S. Antonello, F. Formaggio, C. Toniolo, F. Maran, manuscript in preparation.
[34] D. Seebach, J. L. Mathews, *Chem. Commun.* **1997**, 2015.
[35] R. P. Cheng, S. H. Gellman, W. F. DeGrado, *Chem. Rev*. **2001**, *101*, 3219.
[36] S. Antonello, F. Maran, *J. Am. Chem. Soc*. **1997**, *119*, 12595.
[37] S. Antonello, F. Maran, *J. Am. Chem. Soc*. **1999**, *121*, 9668.
[38] C. Toniolo, G. M. Bonora, E. Benedetti, A. Bavoso, B. Di Blasio, V. Pavone, C. Pedone, *Biopolymers* **1983**, *22*, 1335.
[39] G. M. Sheldrick, SHELXS 97, Program for the Solution of Crystal Structures, University of Göttingen, Germany, 1997.
[40] G. M. Sheldrick, SHELXL 97, Program for the Refinement of Crystal Structures, University of Göttingen, Germany, 1997.

Received May 27, 2002